frontiers | Frontiers in Ecology and Evolution

TYPE Original Research
PUBLISHED 17 May 2023
DOI 10.3389/fevo.2023.1178660

OPEN ACCESS

EDITED BY
Xudong Zhu,
Xiamen University, China

REVIEWED BY
Xuguang Tang,
Southwest University, China
Xianglan Li,
Beijing Normal University, China

*CORRESPONDENCE
Yuqiang Li
✉ liyq@lzb.ac.cn

RECEIVED 03 March 2023
ACCEPTED 03 May 2023
PUBLISHED 17 May 2023

CITATION
Niu Y, Li Y, Liu W, Wang X and Chen Y (2023) Effects of environment factors on the carbon fluxes of semi-fixed sandy land recovering from degradation.
Front. Ecol. Evol. 11:1178660.
doi: 10.3389/fevo.2023.1178660

Effects of environment factors on the carbon fluxes of semi-fixed sandy land recovering from degradation

Yayi Niu[1,2,3], Yuqiang Li[1,2,3,4]*, Wei Liu[1,2], Xuyang Wang[1,2,3] and Yun Chen[1,2,3]

[1]Northwest Institute of Eco-Environment and Resources, Chinese Academy of Sciences, Lanzhou, China, [2]University of Chinese Academy of Sciences, Beijing, China, [3]Naiman Desertification Research Station, Northwest Institute of Eco-Environment and Resources, Chinese Academy of Sciences, Tongliao, China, [4]Key Laboratory of Strategic Mineral Resources of the Upper Yellow River, Ministry of Natural Resources, Lanzhou, China

Shrub-dominated ecosystems in the semiarid Horqin Sandy Land are important terrestrial ecosystems, and substantially affect global ecological health and security. However, there have been few studies of climate change's effects on the carbon fluxes (NEE, net ecosystem exchange; R_{eco}, ecosystem respiration; GPP, gross primary productivity) when these ecosystems are recovering from degradation. We used the eddy covariance technique to determine carbon fluxes and climatic conditions in this ecosystem from 2017 to 2021. The semi-fixed sandy land functioned as a carbon sink in wet years (NEE equaled −14.14 and −126.14 g C m^{-2} yr^{-1} in 2019 and 2021, respectively), but was a carbon source in dry years (NEE equaled 48.50 and 51.17 g C m^{-2} yr^{-1} in 2017 and 2020, respectively) and a normal year (NEE equaled 74.66 g C m^{-2} yr^{-1} in 2018). As expected in these usually water-limited ecosystems, water availability (precipitation and soil water content) were the dominant drivers of NEE, R_{eco}, and GPP, but temperature and photosynthetic photon flux density (PPFD) also played important roles in regulating NEE, R_{eco} and GPP in this recovering semi-fixed sandy ecosystem. With future precipitation and temperature increases, and continuing vegetation restoration, carbon sequestration by this ecosystem is expected to increase. Long-term observations will be necessary to reveal the true source and sink intensities and their response to environmental factors.

KEYWORDS

precipitation, net ecosystem exchange, carbon flux, climate change, semi-fixed sandy land, ecosystem restoration

1. Introduction

Human activities have led to unprecedented and devastating global climate change, including altered precipitation patterns, increased temperatures, and an increasing CO_2 concentration (Intergovernmental Panel on Climate Change [IPCC], 2007; Yu et al., 2013). CO_2 plays a major role in Earth's mass and energy budgets, so quantifying ecosystem carbon cycles and carbon budgets is essential for planning a sustainable future (McGuire et al., 2009; Ma et al., 2020). The balance between photosynthesis (GPP, gross primary productivity) and

ecosystem respiration (R_{eco}) determines the net ecosystem exchange (NEE) in terrestrial ecosystems (Lasslop et al., 2010; Schmitt et al., 2010; Zhang et al., 2019). NEE is therefore an indicator of the strength of the carbon sink or source in terrestrial ecosystems, and comprehending the dynamics of NEE and the underlying mechanisms that drive those dynamics is a crucial issue in global change research (Yu et al., 2013). In particular, the division of NEE into GPP and R_{eco}, which depict two of the fundamental mechanisms, provides a process-level, mechanistic explanation of the regional carbon balance (Reichstein et al., 2005; Jassal et al., 2007; Lasslop et al., 2010; Cao et al., 2021).

About 30% of the Earth's surface is covered by arid and semiarid areas (Kefi et al., 2008; Poulter et al., 2014). Ecosystems in these areas are at risk of soil erosion and ecosystem degradation, which result from a combination of climate change, such as an increasing intensity and frequency of extreme climate events such as drought and extreme precipitation (Knapp et al., 2015), and unreasonable human activities, including overgrazing, excessive firewood harvesting, and excessive deforestation (Domingo et al., 2011; Wang et al., 2021). Despite the fact that many studies of carbon fluxes through ecosystems have been conducted in semi-arid areas (Du and Liu, 2013; Hao et al., 2017; Niu et al., 2020; Zhang et al., 2020), we still do not fully understand how these ecosystems function as CO_2 sources or sinks (Huxman et al., 2004; Ma et al., 2007; Zhou et al., 2020; Niu et al., 2021). This is particularly true for degraded ecosystems during their recovery. Therefore, further investigation will be required to clarify the carbon budget and its controlling mechanisms for sandy land, and especially whether there are different controls on carbon flows in sandy land and other semiarid ecosystems.

The original landscape of China's Horqin Sandy Land was a sparse shrubland and grassland with hydrothermal conditions that were adequate to support shrubs, an abundant plant community with a diverse composition, a stable ecosystem structure, and high productivity. However, the disturbance caused by extensive human activities and the cultivation of a large area of land have caused nearly 80% of the region to experience aeolian desertification since the 1980s; after years of effort to combat this desertification, including grazing exclusion using fences, the area of desertification accounted for only 26% of the total area by the end of 2015 (Liu et al., 1996; Zhao et al., 2007; Duan et al., 2019; Li et al., 2019; Niu et al., 2020). The region's ecological environment is extremely fragile and vulnerable to damage (Meng et al., 2008; Zhu et al., 2020). Grassland, cropland, and ecosystems with semi-fixed sands are the main land uses in this study area (Duan et al., 2019; Zhu et al., 2020). Here, we define "semi-fixed sand" as land in a semiarid area that is covered by a sandy soil and that has a vegetation cover that ranges from 30 to 50% (Zhao et al., 2008); thus, although the vegetation cover indicates some stability against future degradation, it means that recovery is still proceeding. Previous research in this area has shown that the recovering sandy grassland ecosystem was a carbon source on an annual scale, whereas a nearby sandy maize cropland ecosystem was a carbon sink, and that the amount of carbon sink in both ecosystems increased with increasing precipitation (Niu et al., 2020, 2021). To the best of our knowledge, the carbon fluxes of the recovering semi-fixed sandy land ecosystem have received little attention (e.g., Hu et al., 2015), so more studies are needed to understand the carbon flux characteristics at the ecosystem scale, especially for semi-fixed sandy land that has been protected by grazing exclusion using fences to allow natural recovery.

Studies have found that numerous meteorological factors can play vital roles in regulating carbon fluxes (NEE, GPP, and R_{eco}) (Hu et al., 2010; Papale et al., 2015; Tang et al., 2018; Zhang Q. et al., 2018; Watham et al., 2021). For example, the photosynthetic photon flux density (PPFD), air and soil temperatures, precipitation (PPT), soil water content (SWC), and vapor-pressure deficit (VPD) strongly controlled the dynamics of ecosystem carbon fluxes (Jia et al., 2014, 2016; Biederman et al., 2018; Liu et al., 2019). However, the availability of water is generally the main constraint that affects the carbon flux characteristics in water-limited ecosystems (Fu et al., 2006; Zhang et al., 2019; Niu et al., 2020, 2021; Zhou et al., 2020). Thus, water-related parameters such as PPT, SWC, and VPD control the variations in carbon fluxes at different temporal scales (Noormets et al., 2010; Gao et al., 2012; Jia et al., 2014; Niu et al., 2020). Both GPP and R_{eco} may be limited by low water availability (Yuan et al., 2010; Zhou et al., 2013; Zhang Q. et al., 2018; Zhang T. et al., 2018). Decreases of GPP result from limitations on plant physiological processes and alterations of plant phenology (Meir and Woodward, 2010; Zhou et al., 2013), whereas decreases of R_{eco} result from decreased root respiration (Linn and Doran, 1984; Bouma et al., 1997; Lee et al., 2003), decreased soil microorganism activity (Skopp et al., 1990; Drenovsky et al., 2004), and decreased decomposition of organic matter (Liu et al., 2009; Moyano et al., 2012; Cuevas et al., 2013; Wang et al., 2014). Therefore, quantifying how precipitation affects soil water regimes, and how these changes influence NEE, GPP, and R_{eco}, is critical to evaluate the vulnerability of sandy land ecosystems to climate change, and this evaluation will support the development of strategies to preserve or restore these sandy lands (Zhang et al., 2019; Niu et al., 2020).

In this paper, we concentrated on carbon fluxes (NEE, R_{eco}, and GPP) from 2017 to 2021 in a recovering semi-fixed sandy land ecosystem in Inner Mongolia, China. First, there has been little research in our study area, which is an important ecological area of China. Second, our study was conducted at multiple time scales and thereby revealed changes in the dominant factors that affect NEE in response to changes in the time scale. We emphasized carbon flux changes in semi-fixed sandy land ecosystems during the period of recovery from severe desertification, which is a period that has received insufficient attention in the literature. The study area became severely desertified due to excessive reclamation for agriculture and overgrazing. A series of grazing exclosures were erected in 2005 to provide protection against further damage and restore the functions of the degraded ecosystem, which is still recovering from its degradation. Previous research demonstrated that grazing exclosures can increased soil organic carbon and nitrogen and increased the plant species richness, thereby improving a degraded ecosystem's carbon sequestration capacity (Witt et al., 2009; Wang et al., 2017; Adem et al., 2020). However, we still do not know whether the restored ecosystem in our study area is a carbon source or sink and do not fully understand the characteristics of its carbon fluxes. Exploring the characteristics of these fluxes and the influencing factors would provide important information for assessing the vulnerability of degraded semi-fixed sandy land ecosystems.

On this basis, we had three main goals for the present study: (1) To quantify the inter-annual, seasonal, and monthly changes of the three carbon fluxes (NEE, R_{eco}, and GPP). We hypothesized that

the semi-fixed sandy land ecosystem would be a carbon source at the annual scale because the ecosystem is still recovering from its degradation and therefore has low carbon sink capacity (Niu et al., 2020). (2) To identify the environmental variables that control these variations at the three time scales. (3) To identify the impact of water availability (with PPT and SWC used as proxies for water availability to plants) on the carbon fluxes. For goals 2 and 3, we hypothesized that moisture variables would be most important given the semi-arid environment, and would act through their differential effects on plant photosynthesis and soil respiration (Niu et al., 2020, 2021; Zhou et al., 2020), but that other environmental variables would also be important because of their differential effects on plant photosynthesis and soil respiration (Zhou et al., 2020). Previous studies have shown that carbon fluxes in semiarid ecosystems are sensitive to precipitation changes because water availability strongly controls plant growth by controlling carbon uptake and release (Potts et al., 2006; Wang et al., 2014; Scott et al., 2015; Tang et al., 2018; Zhang et al., 2019, 2020). For example, water availability was the dominant factor that influenced carbon fluxes in a sandy maize cropland (precipitation and irrigation) and in a sandy grassland ecosystem (precipitation and the magnitude of the effective precipitation pulses) in our study region (Niu et al., 2020, 2021).

2. Materials and methods

2.1. Site description

Our research was conducted at the Horqin Sandy Land in Naiman Banner, Tongliao City, Inner Mongolia, China (42° 55′N, 120° 42′ E, 377 m a.s.l.; **Figure 1**). The climate is a temperate continental semiarid monsoon climate, with an average annual temperature of 6.8°C and monthly mean values ranging from -9.6°C in January to 24.6°C in July. The mean annual precipitation was 360 mm, and most of the annual precipitation (70%) occurs from May to September (based on data from 1960 to 2014 at the Naiman meteorological station; Niu et al., 2020, 2021). The soils at our study site are a chestnut soil and an aeolian sandy soil (Zhao et al., 2007; Niu et al., 2020). The soil texture of the topsoil (to a depth of 20 cm) is 92% coarse sand, 2% fine sand, and 6% clay. The soil pH was 7.42, soil organic carbon content was 2.47 g kg^{-1}, the bulk density was 1.66 g cm^{-3}, the total nitrogen content was 0.16 g kg^{-1}, and the field moisture capacity was 24.5%. Vegetation cover ranged from 30 to 50%, and was dominated by *Caragana microphylla* in the shrub layer, and the herbaceous species included *Setaria viridis*, *Pennisetum centrasiaticum*, *Chloris virgata*, and *Artemisia scoparia*.

2.2. Micrometeorological and carbon fluxes measurements

We measured PPFD, air temperature (T_a), precipitation (PPT), the soil water content (SWC), and the soil temperature (T_s) at four depths (10, 30, 50, and 80 cm). We used the eddy covariance method to determine the CO_2 flux at half-hourly intervals from 2017 to 2021. **Table 1** summarizes the characteristics of the eddy covariance system and the meteorological instruments. Data collection and regular calibration of the eddy covariance flux measurement system followed accepted guidelines (Lee et al., 2006). We screened out nighttime NEE values that were recorded with insufficient turbulent flow using a friction-velocity filter ($u^* < 0.1$ m s^{-1}, the friction-velocity filter provided by the instrument's software; Zhu et al., 2006; Scott et al., 2009). We estimated the daytime ecosystem respiration by extrapolation from the parameterization derived based on the observed relationship between nighttime respiration and temperature, which was then used to separately derive daytime GPP and R_{eco} (Lloyd and Taylor, 1994). For a more detailed description of the eddy covariance data processing (10 Hz raw data, 30-min data quality, and gap-filling methods), see Niu et al. (2020, 2021). We used the degree of energy closure to assess the data quality of the eddy covariance system (Wilson et al., 2002). The energy closures ranged from 0.58 to 0.67 throughout our study (**Supplementary Figure 1**), indicating that the data observed at our study site met the requirements for a reliable observation, which comprises a closure between 0.56 and 0.97 (Wilson et al., 2002; Niu et al., 2021).

2.3. Random Forest and statistical analyses

We used the Random Forest analysis model (Pham and Brabyn, 2017) [we used version 4.7-1.1 of the randomForest package for the R software (cran.r-project:web/packages/randomForest/index.html) for this analysis] to identify the main factors that influenced the seasonal NEE, R_{eco}, and GPP (mean daily fluxes) for the meteorological factors (PPT, PPFD, T_a, VPD, and the T_s and SWC at four depths). Because the root system of the natural *C. microphylla* shrubs in our study area is mainly found above a depth of 80 cm (A et al., 2003), we measured the SWC and T_s at depths of 10, 30, 50, and 80 cm to cover the full rooting zone. Random Forest is a popular machine-learning algorithm that is used for both classification and regression. The fit of each "tree" in the "forest" is evaluated by using randomly selected points that include 2/3 of the original dataset in a bootstrap sample for training and retain the remaining 1/3 of the dataset for validation. The importance of each factor is determined by the magnitude of the increase in the residual variance when values of the dependent variables are permuted. Random Forest models are also simple to train, can handle a large amount of mixed-type data, and provide ways to evaluate variable importance scores (Pham and Brabyn, 2017). We also assessed the stability and generalization of the model and the cross-validated goodness of fit (R^2) and the root-mean-square error (RMSE). We set the analytical parameters to 1,000 decision trees (ntree), 5 random subsets of the predictors (mtry), and a node size of 5 (Pham and Brabyn, 2017; Zhou et al., 2020; Niu et al., 2021).

For the data analysis at monthly and annual scales, we determined the relationships between the climatic factors and the carbon fluxes using correlation analysis (Pearson's r). We used version 22.0 of the SPSS software[1] to perform all descriptive

1 www.ibm.com/spss

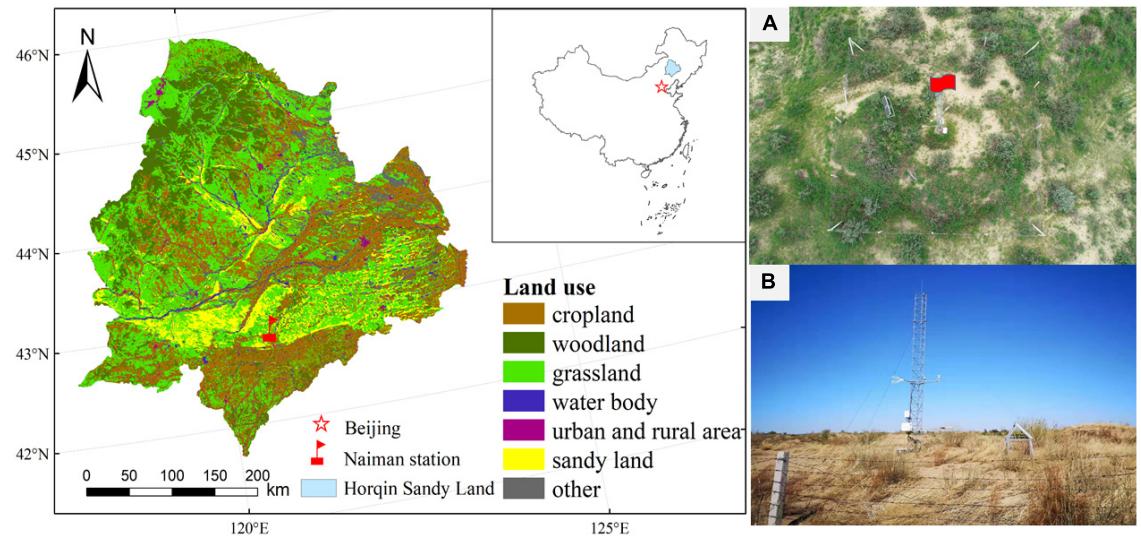

FIGURE 1
Location of the study area and its land uses. **(A,B)** are photos of the observation site during the growing season and dormant season, respectively.

TABLE 1 Characteristics of the eddy covariance system and the meteorological instruments and their positions at our study site in the semi-fixed sandy land ecosystem.

Instrument	Model and manufacturer	Position (cm above the surface)
CO_2/H_2O fluxes	EC150, Li-Cor, Lincoln, NE, USA	300
Three-dimensional wind speed detector	CAST3, Campbell Scientific Inc., Logan, UT, USA	300
Datalogger	CR3000, Campbell Scientific	100
Air temperature (T_a) and relative humidity (RH) sensor	HMP45C, Vaisala Inc., Helsinki, Finland	150
Precipitation gauge (PPT)	Tr525, Texas Electronics, Inc., Dallas, TX, USA	200
Photosynthetic photon flux density (PPFD) detector	LI-190SL-10, Li-Cor Inc.	200
Soil temperature and soil water content (T_s and SWC)	Hydra Probe, Stevens Water Monitoring Systems Inc., Portland, OR, USA	−10, −30, −50, −80
Soil heat flux (SHF)	HFP01-10, Hukseflux Inc., Delft, Netherlands	−5, −10

statistics and statistical analyses: correlation analysis, one-way analysis of variance (ANOVA), and regression analysis. When the ANOVA result was significant, we used least-significant-difference (LSD) tests to determine which pairs of values differed significantly. Before the regression analysis, we tested for collinearity; we proceeded with the analysis if the variance inflation factor was VIF < 10. All datasets passed this test. We used version 8.0 of the Origin software (OriginLab Corporation, Northampton, MA, USA) for graphing our results.

3. Results

3.1. Meteorological conditions

The environmental factors showed strong seasonal dynamics from 2017 to 2021 (Figure 2). Temperature (T_a and T_s) and PPFD both exhibited approximately unimodal trends. These parameters were therefore largely stable and did not differ greatly among years (Table 2 and Supplementary Table 1).

The annual cumulative PPT varied greatly during the observation period, and differed between many pairs of years (Figure 2F and Table 2), the PPT values in 2017 and 2020 were less than in a typical year (an average of 360 mm from 1960 to 2014; Niu et al., 2020; wet years, normal years and dry years are divided according to the average annual precipitation, which is generally less than −10% in dry years, −10 to 10% in normal year, more than 10% in wet year), whereas PPT in 2018 was nearly normal and 2019 and 2021 were wetter than normal. SWC followed the same general trend as PPT (Figure 2E and Supplementary Table 1).

Vapor-pressure deficit (VPD) is also related to PPT, but it showed the opposite pattern of SWC. VPD generally showed a unimodal trend, except for minor secondary peaks in 2019 and 2021, which were wetter than the other years (Figure 2A). However, the mean value did not differ significantly among the years, except for a significantly higher value in the dry year 2017 (Table 2).

3.2. Variations in carbon fluxes

Net ecosystem exchange (NEE), R_{eco}, and GPP showed strong seasonal changes associated with cycles of vegetation growth throughout the growing season (from May to September), but

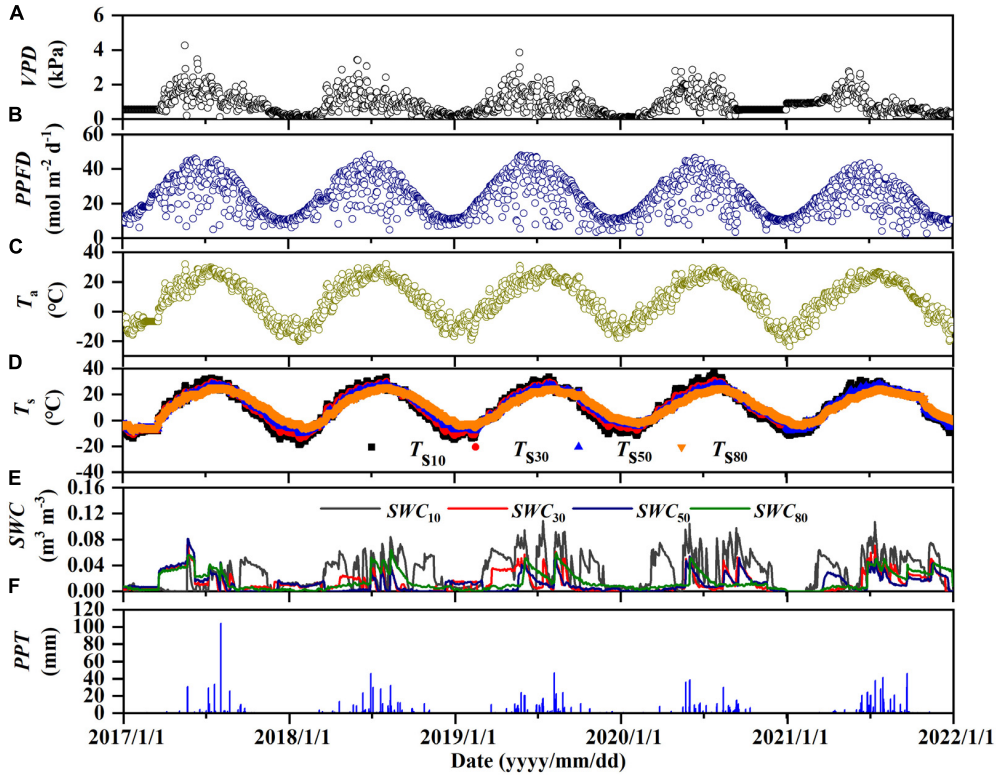

FIGURE 2
Seasonal dynamics of the **(A)** daily average vapor-pressure deficit (VPD), **(B)** photosynthetic photon flux density (PPFD), **(C)** air temperature (T_a), **(D)** the soil temperature (T_s) and **(E)** soil water content (SWC) at depths of 10, 30, 50, and 80 cm, and **(F)** daily precipitation (PPT).

TABLE 2 Annual mean values of the meteorological factors from 2017 to 2021 in the recovering semi-fixed sandy ecosystem.

Year	T_a (°C)	VPD (kPa)	PPFD (mol m^{-2} d$^{-1)}$	PPT (mm)	NEE (g C m^{-2} yr^{-1})	R_{eco} (g C m^{-2} yr^{-1})	GPP (g C m^{-2} yr^{-1})
2017	7.90a	1.00b	24.00a	313	48.50	729.80	681.29
2018	8.03a	0.76a	23.55a	351	74.66	728.37	657.79
2019	8.48a	0.79a	23.86a	382	−14.14	614.20	628.34
2020	8.26a	0.79a	22.62a	312	51.17	571.17	520.00
2021	8.08a	0.83a	21.02a	430	−126.14	680.37	806.51
Mean	8.15	0.83	23.01	358	6.81	664.78	658.79

Values of a variable labeled with the same letter did not differ significantly among the years (ANOVA followed by LSD test). The differences among the years were calculated using the daily averages of the variables. Precipitation (PPT), net ecosystem exchange (NEE), ecosystem respiration (R_{eco}), and gross primary productivity (GPP) represent the cumulative values for the whole year. T_a, air temperature; VPD, vapor-pressure deficit; PPFD, photosynthetic photon flux density; PPT, total precipitation; NEE, net ecosystem exchange; R_{eco}, ecosystem respiration; GPP, gross primary production. The different letters in the same column indicate the significant difference at 5% level.

NEE was generally stable across the years outside the growing season (Figure 3). Daily NEE, R_{eco}, and GPP showed similar seasonal dynamics in all five years, with the ecosystem behaving as a carbon sink during most of the growing season (NEE < 0), but with a few days when it behaved as a carbon source. However, the magnitudes of NEE, R_{eco}, and GPP differed among years (Figure 3A), with higher carbon fluxes in the wet year (2021) and normal precipitation year (2018) than in the dry years (2017 and 2020). We selected 2020 as a representative dry year (Figures 3B, D) and 2021 as a representative wet year (Figures 3C, E), and analyzed the changes of the carbon fluxes under different water conditions during the growing season (with different PPT and different SWC at the four depths). The results showed that the carbon fluxes in the wet year were significantly higher than those in the dry year: NEE was −1.20 versus −0.19 g C m^{-2} d^{-1} for wet and dry years, respectively; the corresponding R_{eco} values were 2.89 versus 2.19 g C m^{-2} d^{-1}, and the corresponding GPP values were 4.09 versus 2.38 g C m^{-2} d^{-1}. All three differences were significant ($P < 0.001$). There are two main reasons for these differences. First, higher precipitation early in the growing season (June; 71.4 mm in 2021 vs. 39.4 mm in 2020) led to higher microbial activity, faster seed germination, and more growth of the plants, thereby increasing carbon fluxes. Second, the high precipitation frequency at the peak of the growing season in

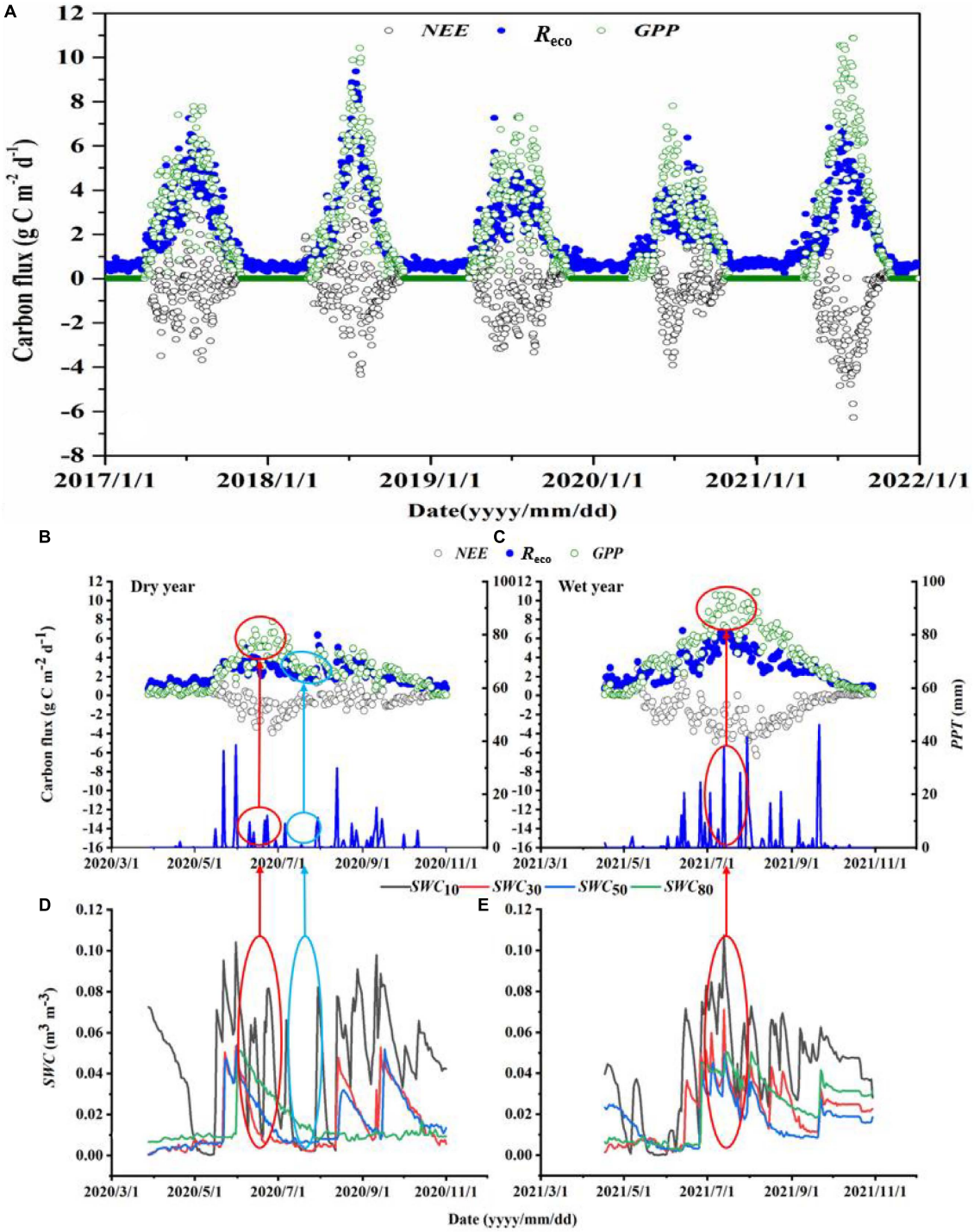

FIGURE 3
(A) Seasonal variability of the daily mean carbon fluxes (NEE, net ecosystem exchange; R_{eco}, ecosystem respiration; GPP, gross primary productivity) from 2017 to 2021. The variations of NEE, R_{eco}, and GPP, and of precipitation (PPT) and soil water content at depths of 10, 30, 50, and 80 cm (SWC_{10}, SWC_{30}, SWC_{50}, and SWC_{80}, respectively) during the growing season in **(B,D)** the dry year (2020) and **(C,E)** wet year (2021). Red circles represent changes in NEE, R_{eco}, and GPP and SWC in response to wet periods during the growing season; the blue circle represents the changes of NEE, R_{eco}, GPP, and SWC during the dry period of the growing season.

the wet year (July; 11 events for a total of 110.2 mm in 2021) greatly promoted the growth of herbaceous and sub-shrub plants. The root system of *C. microphylla* reached a depth of 80 cm, and SWC at 80 cm remained high (0.04 m^3 m^{-3}; Figures 3C, E). This increased the vegetation community productivity. In contrast, during the dry year, the continuous dry conditions at the peak of the growing season (July; 5 events for a total of 14 mm in 2020) significantly damaged or killed the herbaceous plants and thereby rapidly reduced carbon fluxes in the ecosystem (Figures 3B, D).

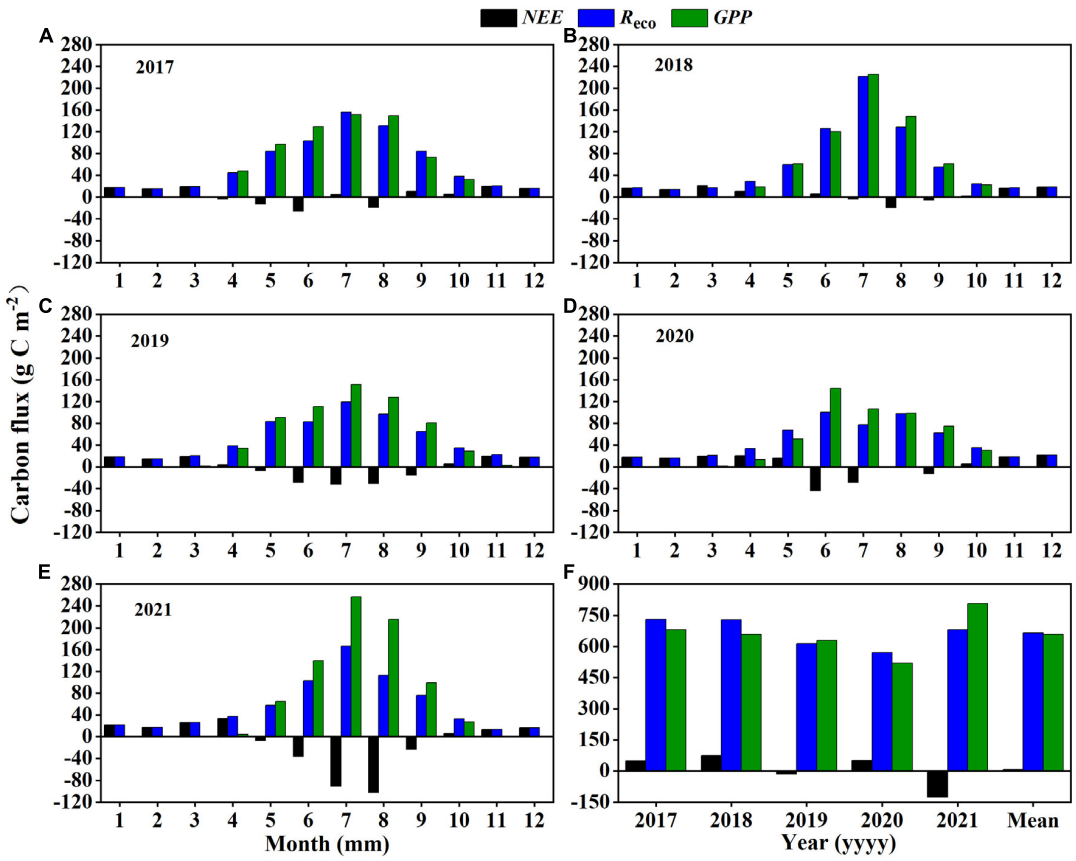

FIGURE 4
(A–E) Monthly and **(F)** inter-annual variations of the cumulative carbon fluxes (NEE, net ecosystem exchange; R_{eco}, ecosystem respiration; and GPP, gross primary productivity) from 2017 to 2021.

At a monthly scale (Figures 4A–E), R_{eco} and GPP generally showed unimodal trends and peaked in July. Due to the influence of PPT and SWC on these fluxes, NEE in the wet years showed carbon absorption throughout the growing season (from May to August in 2019 and 2021; Figures 4C, E and Table 2), whereas in the dry and average years, NEE showed carbon sink in about 3 months and carbon source in the other months (2017, 2018, and 2020; Figures 4A, B, D and Table 2).

At an annual scale (Figure 4F), the mean NEE, R_{eco}, and GPP for all 5 years combined were 6.81 ± 36.35, 664.78 ± 31.49, and 658.79 ± 46.11 g C m^{-2} yr^{-1}, respectively. In the wet years (2019 and 2021), the semi-fixed sandy land showed net carbon sink, with cumulative annual NEE of −14.14 and −126.14 g C m^{-2} yr^{-1}, respectively (Table 2). In contrast, in the dry years (2017 and 2020) and the normal year (2018), the system showed net carbon source, with cumulative annual NEE of 48.50, 51.17, and 74.66 g C m^{-2} yr^{-1}, respectively.

3.3. Responses of NEE, GPP, and R_{eco} to variations in meteorological factors

The environmental factors and NEE were largely stable during the dormant season in all years, so in the rest of this paper, we will concentrate on the relationships between the carbon fluxes and the meteorological factors during the growing season. Figure 5 illustrates the importance values of the variables from the Random Forest analysis, which represent the contributions of the variables to NEE, R_{eco}, and GPP. Supplementary Figure 2 shows the relationships between the measured fluxes and the fluxes predicted using the Random Forest model. For NEE, the most critical variable was PPFD, with an importance of 62.2%, followed by the factors associated with moisture (43.6% for SWC_{80}, 41.9% for SWC_{50}, 40.8% for SWC_{30}, 29.3% for SWC_{10}, and 22.9% for PPT), which were all significant at $P < 0.01$. For R_{eco}, the air temperature (147.7% for T_a) was the most important variables, followed by shallow soil SWC (SWC_{10}) and deep soil SWC (SWC_{80}), with importance values of 76.7 and 73.2%, which were all significant at $P < 0.05$. For GPP, SWC_{80} was the most important factor, with an importance of 92.3%, followed by the factors associated with radiation (79.3 for PPFD), moisture (55.3% for SWC_{30}) and temperature (49.9% for T_{s30}, 40.7% for T_{s50}, and 25.3% for T_{s10}), which were significant at $P < 0.05$.

At the monthly scale, the carbon fluxes (NEE, R_{eco}, and GPP) were significantly correlated with PPFD, temperature (T_a, T_{s10}, T_{s30}, T_{s50}, and T_{s80}), PPT, and deep soil water content (SWC_{30}, SWC_{50}, and SWC_{80}), but were not significantly related to surface soil moisture (SWC_{10}) and VPD (Figure 6 and Table 3). The monthly PPFD, average of the air and soil temperatures (T_{ave}), PPT, and deep soil water content (SWC_{30}, SWC_{50}, and SWC_{80})

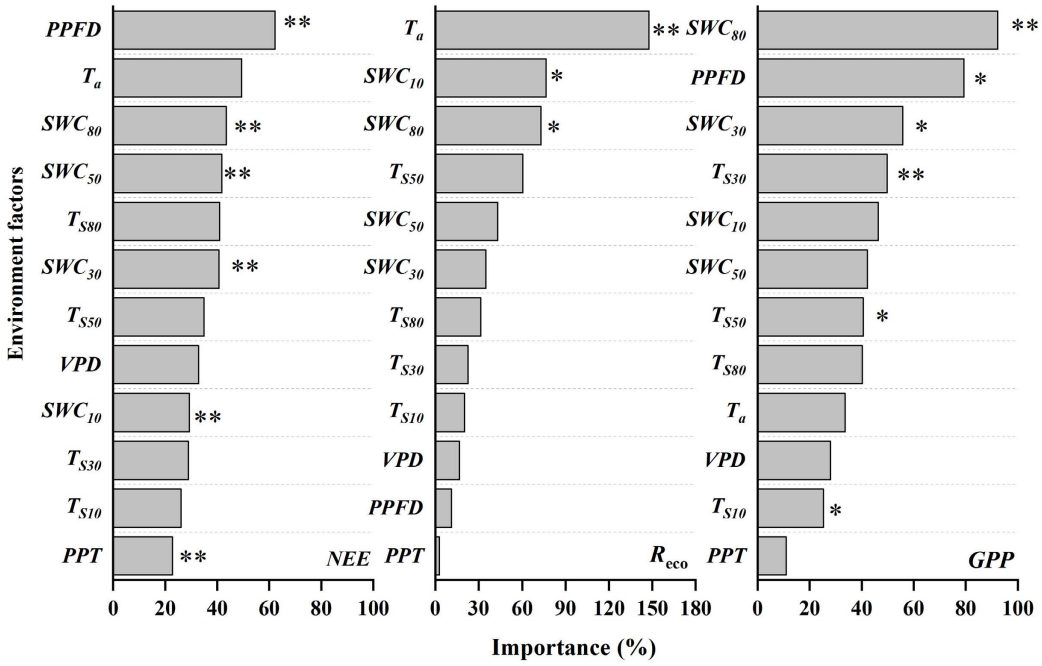

FIGURE 5
Importance values from the Random Forest model analysis for the daily mean carbon fluxes (NEE, net ecosystem exchange; R_{eco}, ecosystem respiration; GPP, gross primary productivity) during the 2017 to 2021 growing seasons. ** and * refer to significance at 0.01 and 0.05, respectively. Variables: PPFD, mean photosynthetic photon flux density; PPT, daily total precipitation; T_a, mean air temperature; T_s and SWC, mean soil temperature and water content at depths of 10, 30, 50, and 80 cm; VPD, mean vapor-pressure deficit.

were significantly negatively correlated with NEE but significantly positively correlated with GPP and R_{eco} (Figure 6), and GPP responded more strongly than R_{eco} to these factors: for the linear relationships in Figure 6, $slope_{GPP} > slope_{Reco}$; for the exponential relationships, $regression\ coefficient_{GPP} > regression\ coefficient_{Reco}$. That is, plants were affected more strongly than soil microbes by changes of PPFD, temperature, and water availability.

At the yearly scale, the mean PPFD, the T_a, the T_s at all depths, and VPD were relatively stable across the study period, and the relationships between these environment factors and the NEE, R_{eco}, and GPP were not significant. The main environmental variation during the study period was the availability of water, which is reflected by PPT and the SWC at all depths (Figure 2 and Table 2). We found that NEE was strongly negatively correlated with PPT, but not significantly related to the other environmental factors (Table 4); conversely, R_{eco} did not have a significant relationship with any of the environmental conditions, and GPP was significantly positively related with PPFD and SWC_{80}. That is, the ecosystem's carbon sequestration capacity rose when PPT, PPFD, and SWC_{80} increased.

4. Discussion

4.1. Comparison with other dryland ecosystems

The NEE of the recovering semi-fixed sandy land ecosystem in our study area changed greatly, from carbon sink to carbon source, in responses to changes in the water availability, which agrees with previous studies of dryland ecosystems (Mielnick et al., 2005; Liu et al., 2012). Our study showed that the semi-fixed sandy land was a net carbon source in dry years, and a weak carbon sink in relatively wet years. The yearly mean NEE was 6.81 g C m^{-2} yr^{-1} during the study period (Figure 4F and Tables 2, 4). Our results agree with previous findings in dryland ecosystems, which showed that the variability in PPT significantly influenced the carbon fixation of the ecosystem, which is dominated by *C. microphylla* shrubs, leading it to alternate rapidly between carbon sink and carbon source (Jia et al., 2016; Liu et al., 2016). However, the magnitude of the average annual NEE at our site was lower than the magnitudes at grassland and shrub sites with similar PPT and seasonality in other parts of China and in the United States: a mixture of xerophytic shrub species had a mean NEE of −77 g C m^{-2} yr^{-1} (Jia et al., 2014); a phreatophyte-dominated ecosystem in China's Gurbantünggüt Desert ecosystem had an NEE that ranged from −40 to −5 g C m^{-2} yr^{-1} (Liu et al., 2016); a *Lycium andersonii* and *Ambrosia dumosa* shrubland ecosystem had an NEE of −127 g C m^{-2} yr^{-1} (Jasoni et al., 2005); and a mature semi-arid shrub ecosystem in California, United States, that was dominated by *Adenostoma fasciculatum* had an NEE that ranged from −155 to −96 g C m^{-2} yr^{-1} (Luo et al., 2007). A regional synthesis of six eddy covariance sites (33 site-years of measurements) in shrublands of the three warm North American deserts (the Chihuahuan, Sonoran, and Mojave deserts) showed that NEE ranged from −100 to 10 g C m^{-2} yr^{-1} (Biederman et al., 2018). One of the factors contributing to the low NEE at our study site was the fact that the site was recovering from severe degradation, and therefore still had a relatively low vegetation cover (30 to 50%). This difference

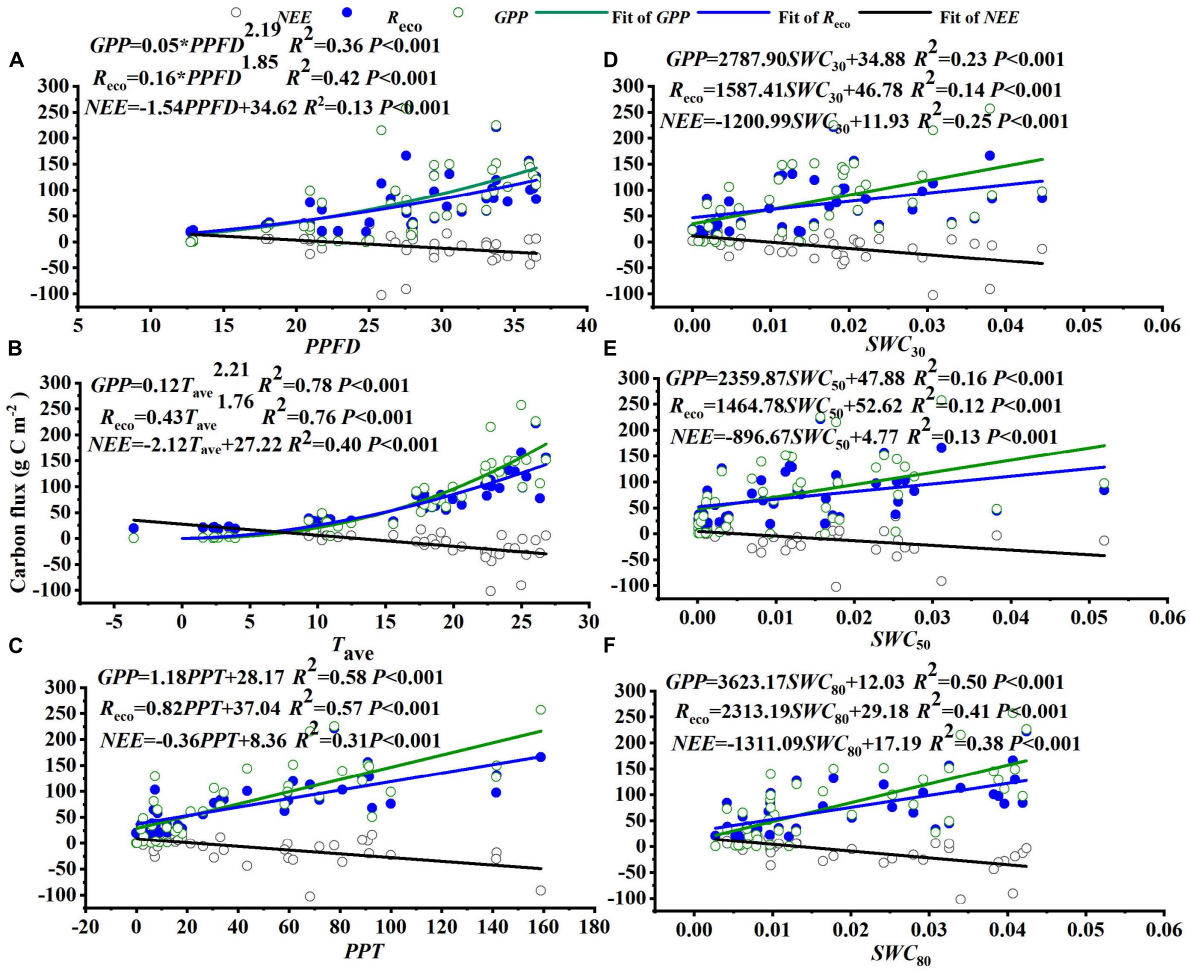

FIGURE 6
Relationships between the monthly net ecosystem exchange (NEE), gross primary productivity (GPP), and ecosystem respiration (R_{eco}) and the **(A)** mean photosynthetic photon flux density (PPFD), **(B)** average temperature (T_{ave}), which represents the average of the air temperature (T_a) and the soil temperature at depths of 10, 30, 50, and 80 cm (T_{s10}, T_{s30}, T_{s50}, and T_{s80}) based on the results of a collinearity test, **(C)** total monthly precipitation (PPT), and **(D–F)** mean soil water contents at depths of 30, 50, and 80 cm (SWC_{30}, SWC_{50}, and SWC_{80}, respectively) during the growing season.

TABLE 3 The results of the correlation analysis (Pearson's *r*) for the relationships between the monthly carbon fluxes (NEE, net ecosystem exchange; R_{eco}, ecosystem respiration; and GPP, gross primary production) and the potential drivers from 2017 to 2021 during the growing season.

	Pearson's *r*										
Carbon flux	VPD	PPFD	PPT	T_a	T_{s10}	T_{s30}	T_{s50}	T_{s80}	SWC_{10}	SWC_{30}	SWC_{50}	SWC_{80}
NEE	−0.04	−0.39**	−0.57**	−0.63**	−0.63**	−0.63**	−0.65**	−0.62**	−0.22	−0.54**	−0.38*	−0.61**
R_{eco}	0.33*	0.65**	0.76**	0.85**	0.83**	0.82**	0.82**	0.78**	0.07	0.43**	0.34*	0.60**
GPP	0.25	0.62**	0.77**	0.86**	0.84**	0.84**	0.84**	0.80**	0.14	0.53**	0.40**	0.68**

Significance: *$P < 0.05$; **$P < 0.01$. PPFD (mol m^{-2} d^{-1}), photosynthetic photon flux density; PPT (mm), total precipitation; SWC (m^3 m^{-3}) and T_s (°C), soil water content and soil temperature at depths of 10, 30, 50, and 80 cm, respectively; T_a (°C), air temperature; VPD (kPa), vapor-pressure deficit.

is a novel result because few previous studies examined recovering sites.

As expected, water availability (the magnitude and timing of precipitation and the SWC at different depths) were the dominant drivers of carbon fluxes in the water-limited ecosystem at our study site (**Figures 3**, **4**, **6**). However, desertification as a result of ecosystem degradation in the study region could have significantly decreased soil carbon storage (mainly due to the loss of nutrient-rich fine soil particles that were eroded by wind) and low soil productivity (because plant and litter carbon storage would have decreased as the vegetation cover, biodiversity, and land productivity decreased during ecological degradation) in the ecosystem at our study site (Feng and Xing, 2008; Zhou et al., 2008; Tang et al., 2015). Desertification can also seriously damage the carbon balance of an ecosystem, leading the carbon emission by soil respiration to exceed the carbon absorption by plants. In

TABLE 4 The results of correlation analysis (Pearson's *r*) for the relationships between the mean annual carbon fluxes (NEE, net ecosystem exchange; R_{eco}, ecosystem respiration; and GPP, gross primary production) and the potential drivers from 2017 to 2021.

	Pearson's *r*											
Carbon flux	PPT	VPD	PPFD	T_a	T_{s10}	T_{s30}	T_{s50}	T_{s80}	SWC_{10}	SWC_{30}	SWC_{50}	SWC_{80}
NEE	−0.89*	0.06	−0.32	−0.14	−0.69	−0.67	−0.63	−0.63	−0.43	−0.65	−0.46	−0.80
R_{eco}	0.06	0.46	0.74	−0.82	−0.57	−0.60	−0.65	−0.55	−0.69	0.12	0.16	0.45
GPP	0.74	0.26	0.76*	−0.45	0.15	0.11	0.05	0.12	−0.13	0.58	0.45	0.93*

Significance: *$P < 0.05$. PPFD, photosynthetic photon flux density (mol m^{-2} d^{-1}), PPT (mm), total precipitation; SWC (m^3 m^{-3}) and T_s (°C), soil water content and soil temperature at depths of 10, 30, 50, and 80 cm, respectively; T_a (°C), air temperature; VPD (kPa), vapor-pressure deficit.

this case, the soil organic carbon pool becomes a backup carbon source for soil respiration that compensates for the lack of carbon sequestration and litterfall by plants.

To promote the recovery of a desertified ecosystem such as the one at our study site, managers should promote vegetation restoration and recovery of the ecosystem (Zhao et al., 2009). However, the carbon sequestration capacity of the recovering semi-fixed sandy land ecosystem was higher than that of another recovering sandy grassland in our study region that was dominated by herbaceous species, which had an average annual NEE of 49 g C m^{-2} yr^{-1} from 2015 to 2018 (Niu et al., 2020). A plausible explanation for the difference between the two areas relates to differences in the vegetation types and differences in their vegetation cover and biomass. Zhang (2007) demonstrated that the carbon fixation capacity of *C. microphylla* was higher than that of herbaceous and sub-shrub plants such as *Artemisia frigida* at the previous study site in the Horqin Sandy Land.

4.2. Impacts of environmental conditions on carbon fluxes

Carbon fluxes are influenced by a variety of environmental factors in complicated and interacting ways, and the main control factors change substantially across time scales (Fu et al., 2009; Niu et al., 2010; Zhang Q. et al., 2018). At a seasonal scale, our Random Forest results showed that PPFD and deep SWC (SWC_{80}) were the most important environmental drivers for GPP and NEE (**Figure 5**), which suggests that light and soil water stress were limiting photosynthetic activity. As the main energy source for photosynthesis, PPFD plays an important role in plant carbon fixation, so with increasing PPFD, an ecosystem's carbon sequestration capacity generally increases (Zhou et al., 2020; Niu et al., 2021).

Our results also demonstrated that deep SWC (SWC_{80}) affected the seasonal variation of NEE and GPP (**Figure 5**), since the deep SWC would be closely linked to large precipitation pulses; for example, PPT > 20 mm caused synchronous increases in SWC_{80} in our study (**Supplementary Figure 3**). This is because the larger amount of precipitation can infiltrate more deeply into the soil and replenish the deep soil moisture, where it becomes plant-available and can sustain net photosynthesis (Niu et al., 2020). This result was similar to previous studies in dryland ecosystems (Austin et al., 2004; Kurc and Small, 2007; Tang et al., 2018). For seasonal R_{eco}, shallow SWC (SWC_{10}) was the most important factor, followed by deep SWC (SWC_{80}) (**Figure 5**). Smaller rainfall events (PPT < 20 mm; **Supplementary Figure 3**) may alter the shallow SWC and increase microbial respiration at this depth (Thomey et al., 2011); the duration and extent of the microbial metabolic reaction appear to be tightly linked with the availability of shallow soil water content (Huxman et al., 2004). In addition, large rainfall pulses (PPT > 20 mm; **Supplementary Figure 3**) trigger plant root activity in deeper soil layers (Potts et al., 2006). These findings suggest that precipitation mainly affects carbon fluxes (NEE, R_{eco}, and GPP) at a seasonal scale by affecting SWC in the different soil layers in our research ecosystem.

At a monthly scale, the mean temperature (T_{ave}), water availability (PPT and SWC), and PPFD all played an important role in determining when photosynthesis led to net uptake of CO_2 (**Figure 6**). GPP and R_{eco} increased with increases of these factors (**Table 3**). Appropriate temperature, radiation, and water availability will promote photosynthesis and increase carbon fixation of plants (Georgieva and Yordanov, 1993; Huxman et al., 2004; Lin et al., 2005). Plants can increase their photosynthetic rates in response to environmental factors by increasing leaf-level CO_2 exchange, adding more leaf area, or through a combination of both responses (Liu et al., 2012; Hao et al., 2013; Niu et al., 2020, 2021). In contrast, temperature and water availability (PPT and SWC) are the primary regulators of ecosystem respiration (Helbling et al., 2003; Kelsey et al., 2011; Zhang T. et al., 2018; Chang et al., 2021). In addition, root activity regulates the decomposition of soil organic matter and can release root exudates that sustain soil microbes, so its influence on the soil microbial community can limit or increase R_{eco} (Moyano et al., 2012; Wang et al., 2014). The soil temperature and water availability can also increase microbial activity, root respiration, and soil enzyme decomposition of organic matter (Jassal et al., 2008; Wang et al., 2014). The soil temperature, water availability (PPT and SWC), and PPFD influence GPP and R_{eco} differently, so changing the balance between production and respiration will change the monthly NEE (Hao et al., 2013; Niu et al., 2020, 2021). Our results are similar to previous research (Niu et al., 2020, 2021): GPP was more sensitive than R_{eco} to changes in PPT (**Figure 6**). State-of-the-art climate models predict increases in the frequency and intensity of heavy precipitation events and rising temperatures in the future in our study region (Frank et al., 2015). Our results suggest that the amount of carbon sequestration in a semi-fixed sandy ecosystem such as the one at our study site will increase in response to the increasing precipitation and temperature (Lu et al., 2013).

At the annual timescale, PPT was the dominant factor that regulated the annual NEE in our semi-fixed sandy land. NEE was strongly and significantly negatively correlated with PPT

on an annual basis during the study period (Table 4). Most previous studies showed that the magnitude and frequency of precipitation were important factors in regional climate change, as these factors affect biological processes at an ecosystem level (Liu et al., 2012; Hao et al., 2013). Greater rainfall would allow for higher stomatal conductance, leading to higher photosynthesis and leaf area (Harper et al., 2005; Ford et al., 2008; Novick et al., 2016; Niu et al., 2020). However, photosynthesis and biomass production also alter ecosystem respiration processes by affecting substrate availability to support soil microbial respiration (Epstein et al., 1997; Hao et al., 2013; Shi et al., 2014; Niu et al., 2020).

In summary, the three carbon fluxes (NEE, R_{eco}, and GPP) were not affected by single factors, but rather by different combinations of environmental parameters. However, at longer time scales, the important factors that affect the changes of NEE, R_{eco}, and GPP tend to converge on a smaller number of factors. At a daily timescale, their values were influenced primarily by radiation, temperature, and water, but at the monthly and annual timescale, the primary governing factor changed to water availability. Generally, water performed a key role in the change of ecosystem carbon fluxes at all time scales in our semi-arid study region.

5. Conclusion

We studied the carbon fluxes and their environmental driving factors at different time scales in a semi-fixed sandy land that is undergoing restoration to promote its recovery from ecological degradation and to combat desertification in the Horqin Sandy Land. We found that the carbon source or sink intensity of the ecosystem varied among years, largely in response to changes in water availability but also in response to interactions with other environmental variables. The fact that the ecosystem sometimes behaved as a net carbon source confirms our first hypothesis. We also confirmed our second hypothesis that water availability would play a crucial role in ecosystem carbon fluxes, but that other environmental variables would also be important because of their differential effects on photosynthesis and soil respiration. In the wet years (2019 and 2021), the semi-fixed sandy land was a carbon sink, whereas in the dry years (2017 and 2020) and the normal year (2018), the system was a carbon source, with a mean annual NEE of 6.81 g C m^{-2} yr^{-1} during the five years of our study. Although the magnitude of NEE was less than that in many previous studies, this can be explained by the fact that the study site is still recovering from severe degradation. Water availability and the air and soil temperatures played key roles in the changes of ecosystem carbon fluxes in our semi-fixed sandy land ecosystem. If precipitation and temperature increase in the future, as some models predict, vegetation will continue to recover and the ecosystem's potential carbon sequestration is likely to increase.

Data availability statement

The original contributions presented in this study are included in the article/**Supplementary material**, further inquiries can be directed to the corresponding author.

Author contributions

YL, YN, WL, XW, and YC designed the study. YN analyzed the data and drafted the manuscript. All authors had a chance to review the manuscript, contributed to discussion and interpretation of the data, and approved the submitted version.

Funding

This research was supported by the National Natural Science Foundation of China (grants 31971466 and 32001214) and the National Key Research and Development Program of China (2017YFA0604803 and 2017YFA0604801).

Conflict of interest

The authors declare that the research was conducted in the absence of any commercial or financial relationships that could be construed as a potential conflict of interest.

Publisher's note

Supplementary material

The Supplementary Material for this article can be found online at: https://www.frontiersin.org/articles/10.3389/fevo.2023.1178660/full#supplementary-material

References

A, L. M. S., Jiang, D. M., and Pei, T. F. (2003). Relationship between root system distribution and soil moisture of artificial *Caragana microphylla* vegetation in Sandy land (in Chinese). *J. Soil Water* 17, 79–81. doi: 10.1016/j.jenvman.2020.110802

Adem, A. A., Mekuria, W., Belay, Y., Tilahun, S. A., and Steenhuis, T. S. (2020). Exclosures improve degraded landscapes in the sub-humid Ethiopian highlands: the Ferenj Wuha watershed. *J. Environ. Manage.* 270:110802. doi: 10.1007/s00442-004-1519-1

Austin, A. T., Yahdjian, L., Stark, J. M., Belnap, J., Porporato, A., Norton, U., et al. (2004). Water pulses and biogeochemical cycles in arid and semiarid ecosystems. *Oecologia* 141, 221–235. doi: 10.1016/j.agrformet.2017.11.005

Biederman, J. A., Scott, R. L., Arnoni, J. A. I. I. I., Jasoni, R. L., Litvak, M. E., Moreo, M. T., et al. (2018). Shrubland carbon sink depends upon winter water availability in the warm deserts of North America. *Agric. For. Meteorol.* 249, 407–419. doi: 10.1023/A:1004278421334

Bouma, T. J., Kai, L. N., Eissenstat, D. M., and Lynch, J. P. (1997). Estimating respiration of roots in soil: interactions with soil CO_2, soil temperature and soil water content. *Plant Soil* 195, 221–232. doi: 10.1016/j.scitotenv.2021.145320

Cao, D., Zhang, J. H., Xun, L., Yang, S. S., and Yao, F. M. (2021). Spatiotemporal variations of global terrestrial vegetation climate potential productivity under climate change. *Sci. Total Environ.* 770:145320. doi: 10.1007/s12665-021-09393-0

Chang, Y., Zhang, R., Hai, C., and Zhang, L. (2021). Seasonal variation in soil temperature and moisture of a desert steppe environment: a case study from Xilamuren, inner Mongolia. *Environ. Earth Sci.* 80:290. doi: 10.1007/s10342-013-0703-4

Cuevas, R. M., Hidalgo, C., Payán, F., Etchevers, J. D., and Campo, J. (2013). Precipitation influences on active fractions of soil organic matter in seasonally dry tropical forests of the Yucatan: regional and seasonal patterns. *Eur. J. Forest. Res.* 132, 667–677. doi: 10.1016/j.jaridenv.2011.06.018

Domingo, F., Serrano-Ortiz, P., Were, A., Villagarcia, L., Garcia, M., Ramirez, D. A., et al. (2011). Carbon and water exchange in semiarid ecosystems in SE Spain. *J. Arid Environ.* 75, 1271–1281. doi: 10.1007/s00248-003-1063-2

Drenovsky, R. E., Vo, D., Graham, K. J., and Scow, K. M. (2004). Soil water content and organic carbon availability are major determinants of soil microbial community composition. *Microb. Ecol.* 48, 424–430. doi: 10.1016/j.agee.2013.04.009

Du, Q., and Liu, H. Z. (2013). Seven years of carbon dioxide exchange over a degraded grassland and a cropland with maize ecosystems in a semiarid area of China. *Agric. Ecosyst. Environ.* 173, 1–12. doi: 10.1016/j.scitotenv.2018.09.374

Duan, H. C., Wang, T., Xue, X., and Yan, C. Z. (2019). Dynamic monitoring of aeolian desertification based on multiple indicators in Horqin Sandy Land, China. *Sci. Total Environ.* 650, 2374–2388. doi: 10.1890/0012-9658(1997)078[2628:EOTAST]2.0.CO;2

Epstein, H. E., Lauenroth, W. K., and Burke, I. C. (1997). Effects of temperature and soil texture on ANPP in the U.S. great plains. *Ecology* 78, 2628–2631.

Feng, J. M., and Xing, J. (2008). Impact of desertification on soil and vegetation—a case study of the five banners in the South silinggol league. *J. Xianyang Normal Univ.* 24, 74–77. doi: 10.1139/X08-061

Ford, C. R., Mitchell, R. J., and Teskey, R. O. (2008). Water table depth affects productivity, water use, and the response to nitrogen addition in a savanna system. *Can. J. For. Res.* 38, 2118–2127. doi: 10.1111/gcb.12916

Frank, D., Reichstein, M., Bahn, M., Thonicke, K., Frank, D., Mahecha, M. D., et al. (2015). Effects of climate extremes on the terrestrial carbon cycle: concepts, processes and potential future impacts. *Global Change Biol.* 21, 2861–2880. doi: 10.1016/j.agrformet.2006.02.009

Fu, Y. L., Yu, G. R., Sun, X. M., Li, Y. N., Wen, X. F., Zhang, L. M., et al. (2006). Depression of net ecosystem CO_2 exchange in semi-arid *Leymus chinensis* steppe and alpine shrub. *Agric. For. Meteorol.* 137, 234–244. doi: 10.5194/bgd-6-8007-2009

Fu, Y. L., Zhen, Z. M., Yu, G. R., Hu, Z. M., Sun, X. M., Shi, P. L., et al. (2009). Environmental controls on carbon fluxes over three grassland ecosystems in China. *Biogeosci. Discuss.* 6, 8007–8040. doi: 10.1016/j.agrformet.2012.01.007

Gao, Y. H., Li, X. R., Liu, L. C., Jia, R. L., Yang, H. T., Li, G., et al. (2012). Seasonal variation of carbon exchange from a revegetation area in a Chinese desert. *Agric. For. Meteorol.* 156, 134–142. doi: 10.1016/S0176-1617(11)80955-7

Georgieva, K., and Yordanov, I. (1993). Temperature dependence of chlorophyll fluorescence parameters of pea seedlings. *J. Plant Physiol.* 142, 151–155. doi: 10.1016/j.agee.2013.03.011

Hao, Y. B., Kang, X. M., Wu, X., Cui, X. Y., Liu, W. J., Zhang, H., et al. (2013). Is frequency or amount of precipitation more important in controlling CO_2 fluxes in the 30-year-old fenced and the moderately grazed temperate steppe? *Agric. Ecosyst. Environ.* 171, 63–71. doi: 10.1016/j.agrformet.2017.03.006

Hao, Y. B., Zhou, C. T., Liu, W. J., Li, L. F., Kang, X. M., Jiang, L. L., et al. (2017). Aboveground net primary productivity and carbon balance remain stable under extreme precipitation events in a semiarid steppe ecosystem. *Agric. For. Meteorol.* 240–241, 1–9. doi: 10.1111/j.1365-2486.2005.00899.x

Harper, C. W., Blair, J. M., Fay, P. A., Knapp, A. K., and Carlisle, J. D. (2005). Increased rainfall variability and reduced rainfall amount decreases soil CO_2 flux in a grassland ecosystem. *Glob. Change Biol.* 11, 322–334. doi: 10.1039/9781847552266-00003

Helbling, E. W., Zagarese, H., and Wetzel, R. G. (2003). "Solar radiation as an ecosystem modulator," in *UV Effects in Aquatic Organisms and Ecosystems*, eds E. W. Helbling and H. Zagarese (Cambridge: Royal Society of Chemistry), 3–18. doi: 10.1007/s40333-014-0038-0

Hu, F. L., Shou, W. K., Liu, B., Liu, Z. M., and Busso, C. A. (2015). Species composition and diversity, and carbon stock in a dune ecosystem in the Horqin Sandy land of northern China. *J. Arid Land.* 7, 82–93. doi: 10.1111/j.1365-2486.2008.01582.x

Hu, Z. M., Yu, G. R., Fu, Y. L., Sun, X. M., Li, Y. N., Chen, S. P., et al. (2010). Effects of vegetation control on ecosystem water use efficiency within and among four grassland ecosystems in China. *Glob. Change Biol.* 14, 1609–1619. doi: 10.1007/s00442-004-1682-4

Huxman, T. E., Snyder, K. A., Tissue, D., Leffler, A. J., Ogle, K., Pockman, W. T., et al. (2004). Precipitation pulses and carbon fluxes in semiarid and arid ecosystems. *Oecologia* 141, 254–268. doi: 10.1017/CBO9780511546013

Intergovernmental Panel on Climate Change [IPCC] (2007). *Climate Change 2007. the Physical Science Basis. Summary for Policymakers*. New York: Cambridge University Press. doi: 10.1111/j.1365-2486.2005.00948.x

Jasoni, R. L., Smith, S. D., and Arnone, J. A. (2005). Net ecosystem CO_2 exchange in Mojave desert shrublands during the eighth year of exposure to elevated CO_2. *Glob. Change Biol.* 11, 749–756. doi: 10.1016/j.agrformet.2007.01.011

Jassal, R. S., Black, T. A., Cai, T., Kai, M., Zhong, L., Gaumont-Guay, D., et al. (2007). Components of ecosystem respiration and an estimate of net primary productivity of an intermediate-aged douglas-fir stand. *Agric. For. Meteorol.* 144, 44–57. doi: 10.1111/j.1365-2486.2008.01573.x

Jassal, R. S., Black, T. A., Novak, M. D., Gaumont-Guay, D., and Nesic, Z. (2008). Effect of soil water stress on soil respiration and its temperature sensitivity in an 18-year-old temperate douglas-fir stand. *Glob. Change Biol.* 14, 1305–1318. doi: 10.1016/j.agrformet.2016.07.007

Jia, X., Zha, T., Gong, J. N., Wu, B., Zhang, Y. Q., and Qin, S. G. (2016). Carbon and water exchange over a temperate semi-arid shrubland during three years of contrasting precipitation and soil moisture patterns. *Agric. For. Meteorol.* 228–229. doi: 10.5194/bg-11-4679-2014

Jia, X., Zha, T. S., Wu, B., Zhang, Y. Q., and Gong, J. N. (2014). Biophysical controls on net ecosystem CO_2 exchange over a semiarid shrubland in northwest China. *Biogeosciences* 11, 57–70. doi: 10.1016/j.tpb.2008.09.004

Kefi, S., Rietkerk, M., and Katul, G. G. (2008). Vegetation pattern shift as a result of rising atmospheric CO_2 in arid ecosystems. *Theor. Popul. Biol.* 74, 332–344.

Kelsey, K., Wickland, K. P., and Striegl, R. G. (2011). *Temperature Sensitivity of Boreal Soil Respiration Across a Soil Moisture Gradient*. Washington, DC: AGU doi: 10.1111/gcb.12888

Knapp, A. K., Hoover, D. L., Wilcox, K. R., Avolio, M. L., Koerner, S. E., La Pierre, K. J., et al. (2015). Characterizing differences in precipitation regimes of extreme wet and dry years: implications for climate change experiments. *Glob. Change Biol.* 21, 2624–2633. doi: 10.1029/2006WR005011

Kurc, S. A., and Small, E. E. (2007). Soil moisture variations and ecosystem-scale fluxes of water and carbon in semiarid grassland and shrubland. *Water Resour. Res.* 43, 1–13. doi: 10.1111/j.1365-2486.2009.02041.x

Lasslop, G., Reichstein, M., Papale, D., Richardson, A. D., Arneth, A., Barr, A., et al. (2010). Separation of net ecosystem exchange into assimilation and respiration using a light response curve approach: critical issues and global evaluation. *Glob. Change Biol.* 16, 187–208. doi: 10.1023/A:1026192607512

Lee, M. S., Nakane, K., Nakatsubo, T., and Koizumi, H. (2003). Seasonal changes in the contribution of root respiration to total soil respiration in a cool-temperate deciduous forest. *Plant Soil* 255, 311–318. doi: 10.1007/1-4020-2265-4

Lee, X., Massman, W., and Law, B. (2006). *Handbook of Micrometeorology: a Guide for Surface Flux Measurement and Analysis*. Dordrecht: Springer. doi: 10.1016/j.catena.2018.11.021

Li, Y. Q., Wang, X. Y., Chen, Y. P., Luo, Y. Q., Lian, J., Niu, Y. Y., et al. (2019). Changes in surface soil organic carbon in semiarid degraded Horqin grassland of northeastern China between the 1980s and the 2010s. *Catena* 174, 217–226. doi: 10.1360/04yc0048

Lin, Z., Peng, C., Xu, X., Lin, G., and Zhang, J. (2005). Thermostability of photosynthesis in two new chlorophyll b-less rice mutants. *Sci. China C Life Sci.* 48, 139–147. doi: 10.2136/sssaj1984.03615995004800060013x

Linn, D. M., and Doran, J. W. (1984). Effect of water-filled pore space on carbon dioxide and nitrous oxide production in tilled and nontilled soils. *Soil Sci. Soc. Am. J.* 48, 1267–1272. doi: 10.1007/s10021-019-00379-5

Liu, P., Zha, T. S., Jia, X., Black, T. A., Jassal, R. S., Ma, J. Y., et al. (2019). Different effects of spring and summer droughts on ecosystem carbon and water exchanges in a semiarid shrubland ecosystem in northwest China. *Ecosystems* 22, 1869–1885. doi: 10.1007/s10021-015-9954-x

Liu, R., Cieraad, E., Li, Y., and Ma, J. J. E. (2016). Precipitation pattern determines the inter-annual variation of herbaceous layer and carbon fluxes in a phreatophyte-dominated desert ecosystem. *Ecosystems* 19, 601–614. doi: 10.1016/j.agrformet.2012.04.015

Liu, R., Pan, L. P., Jenerette, G. D., Wang, Q. X., Cieraad, E., and Yan, L. (2012). High efficiency in water use and carbon gain in a wet year for a desert halophyte community. *Agric. For. Meteorol.* 162–163, 127–135. doi: 10.1111/j.1365-2486.2008.01728.x

Liu, W. X., Zhang, Z., and Wan, S. Q. (2009). Predominant role of water in regulating soil and microbial respiration and their responses to climate change in a semiarid grassland. *Glob Change Biol.* 15, 184–195.

Liu, X. M., Zhao, H. L., and Zhao, A. F. (1996). *Characteristics of Sandy Environment and Vegetation in the Horqin Sandy Land*. Beijing: Science Press. doi: 10.2307/2389824

Lloyd, J., and Taylor, J. A. (1994). On the temperature dependence of soil respiration. *Funct. Ecol.* 8, 315–323. doi: 10.1890/12-0279.1

Lu, M., Zhou, X., Yang, Q., Li, H., Luo, Y., Fang, C., et al. (2013). Responses of ecosystem carbon cycle to experimental warming: a meta-analysis. *Ecology* 94, 726–738. doi: 10.1111/j.1365-2486.2006.01299.x

Luo, H., Oechel, W. C., Hastings, S. J., Zulueta, R., Qian, Y., and Kwon, H. (2007). Mature semiarid chaparral ecosystems can be a significant sink for atmospheric carbon dioxide. *Glob. Change Biol.* 12, 386–396. doi: 10.1007/s11104-020-04484-6

Ma, J., Liu, R., Li, C. H., Fan, L. L., Xu, G. Q., and Li, Y. (2020). Herbaceous layer determines the relationship between soil respiration and photosynthesis in a shrub-dominated desert plant community. *Plant Soil.* 449, 193–207. doi: 10.1016/j.agrformet.2007.07.008

Ma, S., Baldocchi, D. D., Xu, L., and Hehn, T. (2007). Inter-annual variability in carbon dioxide exchange of an oak/grass savanna and open grassland in California. *Agric. For. Meteorol.* 147, 157–171. doi: 10.1111/j.1365-2745.2009.01529.x

McGuire, A. D., Euskirchen, E. S., Ruess, R. W., Kielland, K., and Mcfarland, J. (2009). The changing global carbon cycle: linking plant-soil carbon dynamics to global consequences. *J. Ecol.* 97, 840–850. doi: 10.1111/j.1469-8137.2010.03390.x

Meir, P., and Woodward, F. I. (2010). Amazonian rain forests and drought: response and vulnerability. *New Phytol.* 187, 553–557.

Meng, Q. T., Li, Y. L., Zhao, X. Y., Zhao, Y. P., and Luo, Y. Y. (2008). Study on CO_2 release of leaf litters in different environment conditions in the Horqin Sandy Land (in Chinese). *Arid Zone Res.* 25, 519–524. doi: 10.1016/j.jaridenv.2004.06.001

Mielnick, P., Dugas, W. A., Mitchell, K., and Havstad, K. (2005). Long-term measurements of CO_2 flux and evapotranspiration in a Chihuahuan desert grassland. *J. Arid Environ.* 60, 423–436. doi: 10.5194/bg-9-1173-2012

Moyano, F. E., Vasilyeva, N., Bouckaert, L., Cook, F., Craine, J., Curiel Yuste, J., et al. (2012). The moisture response of soil heterotrophic respiration: interaction with soil properties. *Biogeosciences* 9, 1173–1182. doi: 10.1111/j.1469-8137.2007.02237.x

Niu, S. L., Wu, M. Y., Yi, H., Xia, J. Y., Li, L. H., and Wan, S. Q. (2010). Water-mediated responses of ecosystem carbon fluxes to climatic change in a temperate steppe. *New Phytol.* 177, 209–219. doi: 10.1007/s11356-021-15751-z

Niu, Y. Y., Li, Y. Q., Wang, M. M., Wang, X. Y., and Chen, Y. (2021). Variations in seasonal and inter-annual carbon fluxes in a semiarid sandy maize cropland ecosystem in China's Horqin Sandy land. *Environ. Sci. Pollut. Res.* 29, 5295–5312. doi: 10.5194/bg-17-6309-2020

Niu, Y. Y., Li, Y. Q., Yun, H. B., Wang, X. Y., and Liu, J. (2020). Variations in diurnal and seasonal net ecosystem carbon dioxide exchange in a semiarid sandy grassland ecosystem in China's Horqin Sandy Land. *Biogeosciences* 17, 6309–6326. doi: 10.1111/j.1365-2486.2009.01928.x

Noormets, A., Gavazzi, M. J., Mcnulty, S. G., Domec, J. C., Sun, G. E., King, J. S., et al. (2010). Response of carbon fluxes to drought in a coastal plain loblolly pine forest. *Glob. Change Biol.* 16, 272–287. doi: 10.1038/nclimate3114

Novick, K. A., Ficklin, D. L., Williams, C. A., Bohrer, G., Oishi, A. C., et al. (2016). The increasing importance of atmospheric demand for ecosystem water and carbon fluxes. *Nature Clim. Change* 6, 1023–1027. doi: 10.1002/2015JG002997

Papale, D., Black, T. A., Carvalhais, N., Cescatti, A., Chen, J., Jung, M., et al. (2015). Margolis, H. effect of spatial sampling from European flux towers for estimating carbon and water fluxes with artificial neural networks. *J. Geophys. Res. Biogeosci.* 120, 1941–1957. doi: 10.1016/j.isprsjprs.2017.03.013

Pham, L. T. H., and Brabyn, L. (2017). Monitoring mangrove biomass change in Vietnam using SPOT images and an object-based approach combined with machine learning algorithms. *ISPRS J. Photogrammetry Remote Sens.* 128, 86–97. doi: 10.1111/j.1469-8137.2006.01732.x

Potts, D. L., Huxman, T. E., Cable, J. M., English, N. B., Ignace, D. D., Eilts, J. A., et al. (2006). Antecedent moisture and seasonal precipitation influence the response of canopy scale carbon and water exchange to rainfall pulses in a semiarid grassland. *New Phytol.* 170, 849–860. doi: 10.1038/nature13376

Poulter, B., Frank, D., Ciais, P., Myneni, R. B., Andela, N., Bi, J., et al. (2014). Contribution of semi-arid ecosystems to interannual variability of the global carbon cycle. *Nature* 509, 600–603. doi: 10.1111/j.1365-2486.2005.001002.x

Reichstein, M., Falge, E., Baldocchi, D., Papale, D., Aubinet, M., Berbigier, P., et al. (2005). On the separation of net ecosystem exchange into assimilation and ecosystem respiration: review and improved algorithm. *Glob. Change Biol.* 11, 1424–1439. doi: 10.5194/bg-7-2297-2010

Schmitt, M., Bahn, M., Wohlfahrt, G., Tappeiner, U., and Cernusca, A. (2010). Land use affects the net ecosystem CO_2 exchange and its components in mountain grasslands. *Biogeosciences* 7:2297. doi: 10.1002/2015JG003181

Scott, R. L., Biederman, J. A., Hamerlynck, E. P., and Barron-Gafford, G. A. (2015). The carbon balance pivot point of southwestern U.S. semiarid ecosystems: insights from the 21st century drought. *J. Geophys. Res. Biogeosci.* 120, 2612–2624. doi: 10.1029/2008JG000900

Scott, R. L., Jenerette, G. D., Potts, D. L., and Huxman, T. E. (2009). Effects of seasonal drought on net carbon dioxide exchange from a woody-plant-encroached semiarid grassland. *J. Geophys. Res. Biogeosci.* 114:G04004. doi: 10.5194/bg-11-621-2014

Shi, Z., Thomey, M. L., Mowll, W., Litvak, M., Brunsell, N. A., Collins, S. L., et al. (2014). Differential effects of extreme drought on production and respiration: synthesis and modeling analysis. *Biogeosciences* 11, 621–633. doi: 10.2136/sssaj1990.03615995005400060018x

Skopp, J., Jawson, M., and Doran, J. W. (1990). Steady-state aerobic microbial activity as a function of soil water content. *Soil Sci. Soc. Am. J.* 54, 1619–1625. doi: 10.1002/ece3.4587

Tang, Y. K., Jiang, J., Chen, C., Chen, Y. M., and Wu, X. (2018). Rainfall pulse response of carbon fluxes in a temperate grass ecosystem in the semiarid Loess Plateau. *Ecol. Evol.* 8, 11179–11189. doi: 10.1016/j.ecoleng.2015.07.023

Tang, Z., An, H., and Shangguan, Z. (2015). The impact of desertification on carbon and nitrogen storage in the desert steppe ecosystem. *Ecol. Eng.* 84, 92–99. doi: 10.1111/j.1365-2486.2010.02363.x

Thomey, M. L., Collins, S. L., Vargas, R., Johnson, J. E., Brown, R. F., Natvig, D. O., et al. (2011). Effect of precipitation variability on net primary production and soil respiration in a Chihuahuan desert grassland. *Glob. Change Biol.* 17, 1505–1515. doi: 10.5194/bg-11-259-2014

Wang, B., Zha, T. S., Jia, X., Wu, B., Zhang, Y. Q., and Qin, S. G. (2014). Soil moisture modifies the response of soil respiration to temperature in a desert shrub ecosystem. *Biogeosci. Discuss.* 10, 9213–9242. doi: 10.3389/fenvs.2021.633020

Wang, X. Y., Li, Y. Q., Wang, X. Y., Li, Y. L., and Gong, X. W. (2021). Temporal and spatial variations in NDVI and analysis of the driving factors in the desertified areas of northern China from 1998 to 2015. *Front. Environ. Sci.* 9:633020. doi: 10.5846/stxb201508101688

Wang, Y. H., Ma, T. E., Wei, Y. C., Wei, X. R., Shao, M. A., Cheng, J. M., et al. (2017). Influence of grazing exclusion on soil organic carbon and nitrogen mineralization in semiarid grasslands of the Loess Plateau (in Chinese). *Acta Ecol. Sin.* 37, 378–386. doi: 10.1007/s10661-021-08896-4

Watham, T., Padalia, H., Srinet, R., Nandy, S., Verma, P. A., and Chauhan, P. (2021). Seasonal dynamics and impact factors of atmospheric CO_2 concentration over subtropical forest canopies: observation from eddy covariance tower and OCO-2 satellite in Northwest Himalaya. *India. Environ. Monit. Assess.* 193:106. doi: 10.1016/S0168-1923(02)00109-0

Wilson, K., Goldstein, A., Falge, E., Aubinet, M., Baldocchi, D., Berbigier, P., et al. (2002). Energy balance closure at FLUXNET sites. *Agric. For. Meteorol.* 113, 223–243.

Witt, G. B., Nol, M. V., Bird, M. I., and Beeton, R. J. S. (2009). *Investigating Long-Term Grazing Exclosures for the Assessment of Carbon Sequestration and Biodiversity Restoration Potential of the Mulga Lands.* Final report. Australia: University of Queensland. doi: 10.1111/gcb.12079

Yu, G. R., Zhu, X. J., Fu, Y. L., He, H. L., Wang, Q. F., Wen, X. F., et al. (2013). Spatial patterns and climate drivers of carbon fluxes in terrestrial ecosystems of China. *Glob. Change Biol.* 19, 798–810. doi: 10.1016/j.rse.2010.01.022

Yuan, W. P., Liu, S. G., Yu, G. R., Bonnefond, J. M., Chen, J. Q., Davis, K., et al. (2010). Global estimates of evapotranspiration and gross primary production based on MODIS and global meteorology data. *Remote Sens. Environ.* 114, 1416–1431.

Zhang, C. L. (2007). *Photosynthesis and Physiological Features of Different Desert Species in Horqin Sand Land*. Master's Thesis. Beijing: Minzu University of China. doi: 10.1016/j.agrformet.2018.05.005

Zhang, Q., Phillips, R. P., Manzoni, S., Scott, R. L., Oishi, A. C., Finzi, A., et al. (2018). Changes in photosynthesis and soil moisture drive the seasonal soil respiration-temperature hysteresis relationship. *Agric. For. Meteorol.* 259, 184–195. doi: 10.1016/j.agrformet.2018.02.027

Zhang, T., Zhang, Y. J., Xu, M. J., Zhu, J. T., Chen, N., Jiang, Y. B., et al. (2018). Water availability is more important than temperature in driving the carbon fluxes of an alpine meadow on the Tibetan Plateau. *Agric. For. Meteorol.* 256–257, 22–31. doi: 10.1016/j.catena.2020.104845

Zhang, R., Zhao, X. Y., Zuo, X. A., Degen, A. A., Li, Y. L., and Liu, X. P. (2020). Drought-induced shift from a carbon sink to a carbon source in the grasslands of Inner Mongolia. *CATENA* 195:104845. doi: 10.1029/2018JD028419

Zhang, R., Zhao, X. Y., Zuo, X. A., Qu, H., Degen, A. A., Luo, Y. Y., et al. (2019). Impacts of precipitation on ecosystem carbon fluxes in desert-grasslands in Inner Mongolia, China, JGR. *Atmospheres* 124, 1266–1276.

Zhao, H. L., Li, Y. Q., and Zhou, R. L. (2007). Effects of desertification on C and N storages in grassland ecosystem on Horqin sandy land (in Chinese). *Chin. J. Appl. Ecol.* 18:2412.

Zhao, H. L., Li, Y. Q., and Zhou, R. L. (2009). Effects of desertification on soil respiration rate and carbon balance in Horqin sandy grassland (in Chinese). *Acta Pedologica Sin.* 42, 809–816.

Zhao, H. L., Zhao, R. L., Zhao, X. Y., and Zhang, T. H. (2008). Ground discriminance on positive and negative processes of land desertification in Horqin Sand Land (in Chinese). *J. Desert Res.* 28, 8–15. doi: 10.1016/j.foreco.2013.01.007

Zhou, J., Zhang, Z. Q., Sun, G., Fang, X. R., Zha, T. G., McNulty, S., et al. (2013). Response of ecosystem carbon fluxes to drought events in a poplar plantation in Northern China. *For. Ecol. Manage.* 300, 33–42. doi: 10.1016/j.geoderma.2008.04.003

Zhou, R. L., Li, Y. Q., Zhao, H. L., and Drake, S. (2008). Desertification effects on C and N content of sandy soils under grassland in Horqin, northern China. *Geoderma* 145, 370–375. doi: 10.1016/j.jenvman.2020.110556

Zhou, Y. Y., Li, X. R., Gao, Y. H., He, M. Z., Wang, M. M., Wang, Y. L., et al. (2020). Carbon fluxes response of an artificial sand-binding vegetation system to rainfall variation during the growing season in the Tengger Desert. *J. Environ. Manage.* 266:110556. doi: 10.1016/j.scitotenv.2020.139929

Zhu, W. J., Gao, Y., Zhang, H. B., and Liu, L. L. (2020). Optimization of the land use pattern in Horqin Sandy land by using the CLUMondo model and Bayesian belief network. *Sci. Total Environ.* 739:139929. doi: 10.1007/s11430-006-8036-5

Zhu, Z. L., Sun, X. M., Wen, X. F., Zhou, Y. L., Tian, J., and Yuan, G. F. (2006). Study on the processing method of nighttime CO_2 eddy covariance flux data in China FLUX (in Chinese). *Sci. China Ser. D Earth Sci.* 49, 36–46.